

Volumetric Correlation PIV to Measure Particle Concentration and Velocity of Micro Flows

C.V. Nguyen¹, A. Fouras² and J. Carberry¹

¹Department of Mechanical and Aerospace Engineering, Monash University, VIC 3800, Australia
chuong.nguyen@eng.monash.edu.au

²Division of Biological Engineering, Monash University, VIC 3800, Australia

ABSTRACT

Volumetric correlation particle image velocimetry (VCPIV) is a recent technique which measures 3-dimensional 2-component velocity field in a fluid volume. As this technique does not take into account the effect of particle concentration variation throughout the measurement volume, significant measurement errors can occur in when the technique is applied to real flows with non-uniform particle concentrations. An improved VCPIV technique is presented which calculates and corrects for variations in particle concentration. Particle concentrations are calculated using the auto-correlation map, and subsequently the velocities are calculated using the cross-correlation and the measured particle concentration. The results show significant improvement in the accuracy of velocity measurements in addition to the ability to calculate the particle concentration profile.

1. INTRODUCTION

Particle Image Velocimetry (PIV) is a measurement method which produces a velocity field from image pairs of particles moving with the flow. In micro PIV, the whole flow is illuminated and images of particles throughout the depth can be captured. Particles at different z (depth) locations appear differently in the image; if the particle image is approximated as a Gaussian distribution then, as described by Olsen and Adrian [7], the particle image diameter d_e and intensity $I(r, z)$ from a particle at a given z location can be expressed as:

$$d_e^2(z) = M^2 d_p^2 + 5.95(M+1)^2 \lambda^2 f^{\#2} + \frac{M^2 z^2 D_a^2}{(s_0 + z)^2} \quad (1)$$

$$I(r, z) = I_0 \exp\left(\frac{-4\beta^2 r^2}{d_e^2}\right) \quad (2)$$

with

$$I_0 = \frac{J_p D_a^2 \beta^2}{4\pi d_e^2 (s_0 + z)^2} \quad (3)$$

where d_p is the particle real diameter, M the lens magnification, $f^{\#2}$ the lens focal number, D_a the lens aperture diameter, s_0 the lens working distance, λ the wavelength of laser source, J_p the flux of light emitter from the particle and $\beta^2 = 3.67$.

The effect of distance from the focal plane, or the out-of-focus effect, on a particle's image intensity and half width $\sigma_{part} = \frac{d_e}{2\sqrt{2}\beta}$ is shown in Figure 1a. This figure is obtained

using equations (1), (2) and (3) for objective lens of $M=5$, $NA=0.12$, $s_0=14mm$ and particle $d_p=3\mu m$. For the same parameters, the variation of the particle's auto-correlation

intensity and half width σ_{peak} with distance from the focal plane are shown in Figure 1b.

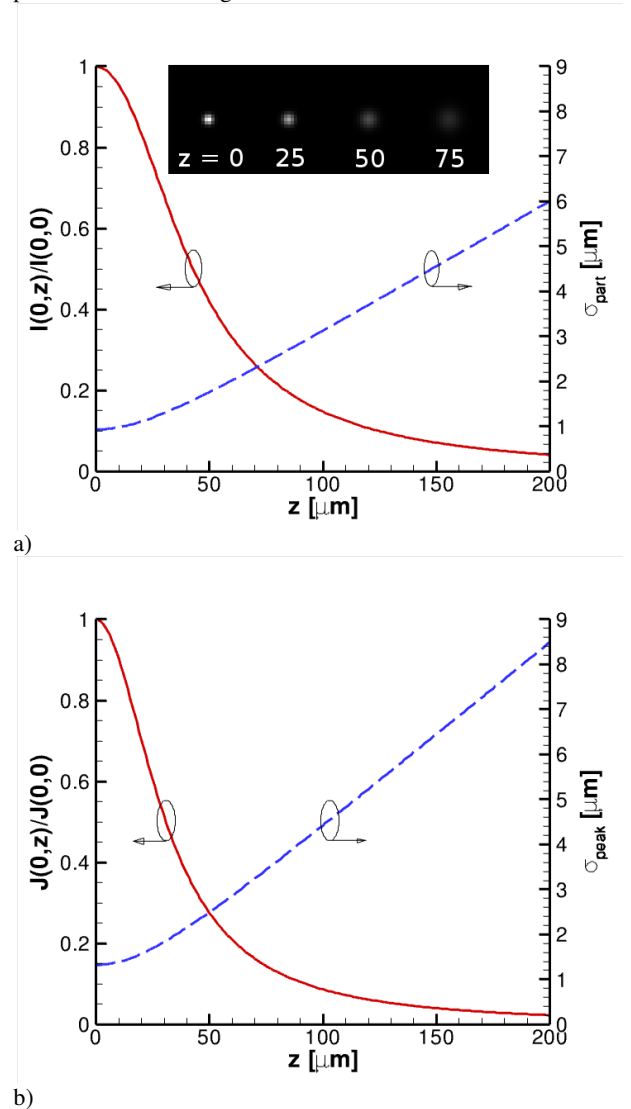


Figure 1. Out-of-focus effect on a) the particles image intensity I , and half width σ_{part} , and b) the intensity J and half width σ_{peak} of the auto-correlation peak of the particles. Intensity (solid curve) and half widths (dashed curve) are shown as functions of z , distance from the focal plane. The inset in figure a) shows the variation of a particle image with z .

In micro PIV the velocity measurements are nominally taken at the focal plane. However, due to the presence of out-of-focus particles within the measurement volume, the measurement contains significant correlation signals, and

therefore measurement bias, from out-of-focus particles. In micro channel flow this measurement bias is greatest in near-wall regions and in the flow centre (Nguyen *et al.* [6]). This bias error has been considered as a major problem (Meinhart *et al.* [5], Olsen and Adrian [7]) and several measurement techniques have been developed to reduce the effect of the out-of-focus particles (Bitsch *et al.* [1], Lindken *et al.* [4], Nguyen *et al.* [6]).

However, the out-of-focus effect in fact can be very useful when being used appropriately. A recent measurement technique, volume correlation PIV (VCPIV) utilizes this phenomenon to measure velocity profile in the z direction from a single correlation peak (Fouras *et al.* [3]). This method is based on the proposition that the full cross-correlation $Cx_{full}(\hat{x}, \hat{y})$ of an image pair containing particles distributed in the z direction is linearly proportional to the summation of the cross-correlations $Cx_{2D}(\hat{x}, \hat{y}, z)$ of the particles at all z positions:

$$Cx_{full}(\hat{x}, \hat{y}) = a \sum_{z=z_1}^{z_N} Cx_{2D}(\hat{x}, \hat{y}, z) + b \quad (4)$$

where a and b are constants and:

$$Cx_{2D}(\hat{x}, \hat{y}, z) = J(0, z) \exp\left(-\frac{(\hat{x} - \delta x)^2 + (\hat{y} - \delta y)^2}{2\sigma_{peak}^2(z)}\right) \quad (5)$$

where $J(0, z)$ is the correlation peak ($r = 0$) intensity of a particle at z location, δx and δy the displacement components in x and y directions of particles at z , $z = z_1$ to z_N is the depth range of particles within the flow.

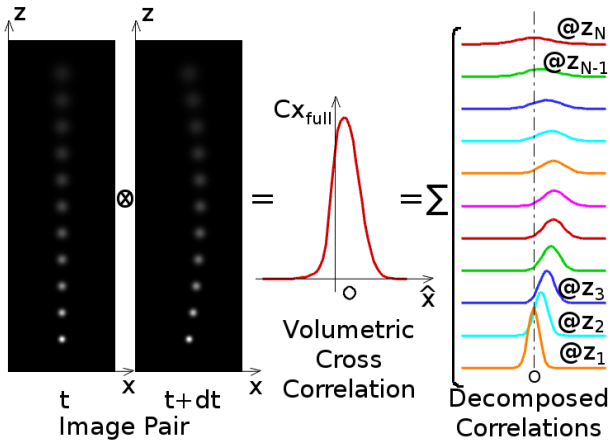


Figure 2. Volumetric correlation and correlation decomposition of a parabolic flow. The correlation of an image pair of particles distributed over the channel depth z yields a full volumetric correlation peak. This peak contains information on both velocity and the out-of-focus effect. To obtain the velocity profile, the volumetric correlation peak is decomposed into correlation peaks at (@) different z positions according to the out-of-focus effect. In this figure, constant particle concentration in the z -direction is assumed.

Velocity measurements are performed by the decomposition of the full correlation into the correlation peaks with velocity at different z locations. An illustration of this process is shown in Figure 2. The displacement components δx and δy in the z direction are obtained using a least-squares solver. The full correlation peak is reconstructed from the auto-correlation peaks of N particles equally spaced in z -direction. For a flow

depth of $100\mu m$, $N = 100$ was found to be sufficient. To reduce the number of degrees of freedom in the velocity component, so that the solver can provide a stable solution, a curve fitting (piece-wise linear or spline) is used to produce the displacement at all z positions and the displacements at the nodes are optimized by the solver. From an image pair divided into several image templates, each of which produces a volumetric correlation peaks, a 3-dimensional 2-component (3D2C) velocity field can be achieved. Typically, to obtain good measurement accuracy, $Cx_{full}(\hat{x}, \hat{y})$ needs to be obtained from the correlation averaging of hundreds or thousands of image pairs.

To improve the optimization speed and accuracy, an optical setup is recommended as shown in Figure 3. To avoid the non-linear part of the σ_{peak} curve the focal plane is located outside the channel at a distance z_0 from the wall, Fouras *et al.* [3].

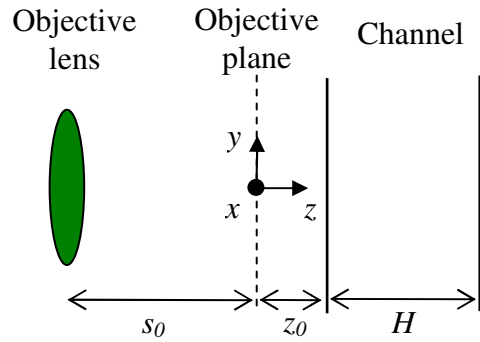


Figure 3. Schematic diagram of the channel (depth H) including coordinate system (adapted from Fouras *et al.*, 2009). The object plane (also the focal plane) is at a working distance s_0 from the objective lens, and at distance z_0 from the channel to avoid the non-linear part of σ_{peak} as shown in Figure 1b. The origin of the coordinates is at the object plane. The principal flow direction is x -direction.

A shortcoming of the volumetric correlation PIV method proposed by Fouras *et al.* [3] is that it does not take into account of the effect of particle concentration. Cao and Wereley [2] showed that in real micro channel flows particle concentration varies significantly, with maximum concentration typically occurring near a location of 0.6 channel radii from the centre, with few particles near walls. The non-uniform particle concentration changes the intensity of correlation in z direction. As a result, the VCPIV measurements produce signification errors when ignoring variations in particle concentration.

2. NEW VOLUMETRIC CORRELATION PIV WITH PARTICLE CONCENTRATION

Using a similar methodology to VCPIV the variation of particle concentration throughout the measurement volume, $C_{part}(z)$ can be described. Our study shows that the magnitude of cross- and auto-correlations is linearly proportional to the number of particles. The effect of non-uniform particle concentration on the correlation peak intensity is shown in Figure 4: with constant concentration the correlation intensity $J(0, z)$ varies as shown by the dash-dash curve, with non-uniform concentration $C_{part}(z)$ shown as a solid curve, the effective correlation intensity $J'(0, z)$ is equal to $C_{part}(z) \times J(0, z)$ as shown as dash-dot curve.

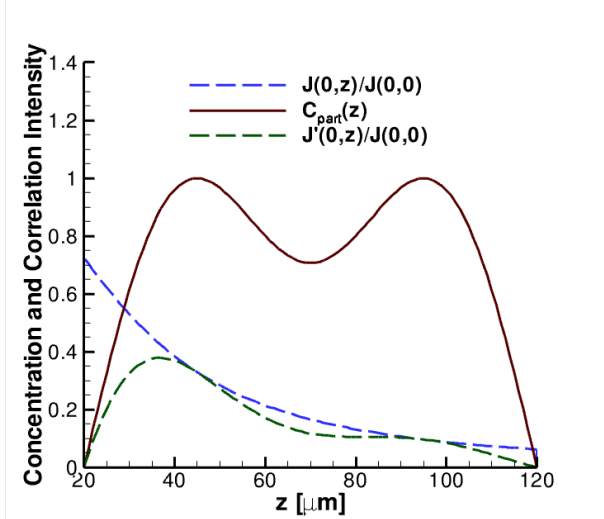


Figure 4. Effect of particle concentration on the mean intensity of the auto-correlation peak within a channel of $100\mu\text{m}$ depth with the focal plane located at $z = 0$. For constant concentration the correlation intensity $J(0,z)$ is as shown by the dash-dot curve. However, with a non-uniform particle concentration $C_{part}(z)$ (solid curve), the effective correlation intensity $J'(0,z) = C_{part}(z) \times J(0,z)$ (dashed-dot).

The cross-correlation function of a particle at a z location is now expressed as:

$$Cx_{2D}(\hat{x}, \hat{y}, z) = J'(0, z) \exp\left(-\frac{(\hat{x} - \delta\hat{x})^2 + (\hat{y} - \delta\hat{y})^2}{2\sigma_{peak}^2(z)}\right) \quad (6)$$

with the effective correlation intensity

$$J'(0, z) = C_{part}(z) \times J(0, z) \quad (7)$$

The particle concentration $C_{part}(z)$ can be computed from the full auto-correlation $Co_{full}(\hat{x}, \hat{y})$ following the same methodology as for velocity:

$$Co_{full}(\hat{x}, \hat{y}) = a \sum_{z=z_1}^{z_N} Co_{2D}(\hat{x}, \hat{y}, z) + b \quad (8)$$

where the 2D auto-correlation:

$$Co_{2D}(\hat{x}, \hat{y}, z) = J'(0, z) \exp\left(-\frac{\hat{x}^2 + \hat{y}^2}{2\sigma_{peak}^2(z)}\right) \quad (9)$$

Using a least-squares solver, $J'(0,z)$, and therefore $C_{part}(z)$, can be obtained the same way as the displacement components $\delta\hat{x}$ and $\delta\hat{y}$. The boundaries of particle distribution in z direction, z_1 and z_N corresponding to the channel walls can also be determined at the same time. This helps simplify the experimental procedures as there is no need to manually locate the wall locations and make measurements in cases where particles do not occupy the whole channel depth. After obtaining $J(0,z)$, the displacement components profile are obtained by solving equation (6), yielding three component velocity.

3. VALIDATION RESULTS AND DISCUSSION

To validate the new VCPIV algorithm, 2048 synthetic image pairs of 1024×1024 pixels size are generated for micro channel flow. The optical setup for synthetic image generation is shown in Figure 3 with $H = 100\mu\text{m}$. The image formation

uses a lens of magnification $M = 5$, numerical aperture $NA = 0.12$, working distance $s_0 = 14\text{mm}$ with the focal plane located $20\mu\text{m}$ outside the channel. Particles of $3\mu\text{m}$ diameter are randomly distributed in the x - y plane and controlled in z direction according to the following function:

$$C_{part}(z) = \sin\left(\frac{z\pi}{H}\right) + \frac{1}{3}\sin\left(\frac{3z\pi}{H}\right), \quad \text{for } 0 \leq z \leq H \quad (11)$$

The concentration profile measured using the new VCPIV method is shown in Figure 5 alongside the exact concentration. The concentration measurement accurately locates the walls, where the concentration is zero, within a sub-micron error. There is a good agreement between the measured and the exact concentration, although there are some discrepancies at the 2nd and 3rd nodes and on the far side of the profile after the 4th node.

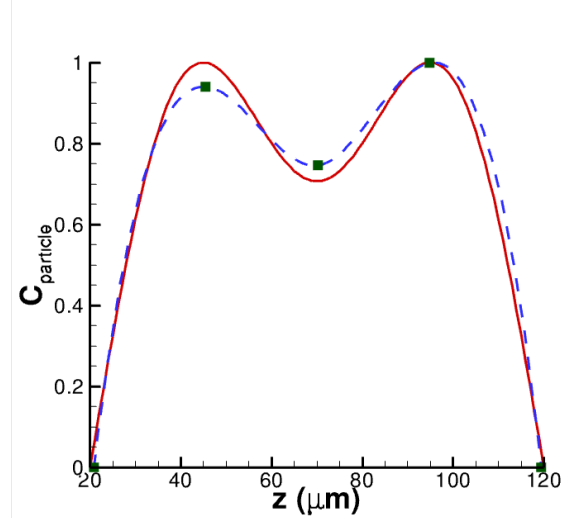


Figure 5. Calculation of particle concentration profile across the measurement depth. Solid line represents the exact solution. Squares represent the nodes for the spline solution (dashed line). The two walls are accurately located within less than $1\mu\text{m}$.

The additional concentration information is now used to correct the velocity measurement. As the flow is symmetrical, the measured concentration profile can also be modified by averaging with its mirror profile to make it symmetrical. Velocity profiles calculated using the measured concentration, the measured symmetrical concentration as well as constant concentration and the exact concentration are shown in Figure 6, and the l^2_{norm} value representing the total measurement error are also shown. Using a constant concentration, Figure 6a, the measured velocity profile is shifted towards the lens and distorted on the far end of the profile. Using the measured concentration without assuming symmetry, Figure 6b, the measurement yields very good agreement with the exact velocity profile, although there are some discrepancies with the exact concentration on the right side of the profile. The measurement error l^2_{norm} is reduced almost 500% compared to that of the measurement using constant concentration. When the measured concentration is assumed to be symmetric, Figure 6c, the measured velocity profile converges very close to the exact profile and the error is further reduced. Finally, using the exact concentration which is never available in real experiments, Figure 6d, as expected the measurement yields excellent agreement with the exact velocity.

4. CONCLUSIONS

The new VCPIV algorithm, which incorporates the effect of particle concentration, is shown to significantly improve the accuracy of velocity measurements, while also providing particle concentration profile with good accuracy. With the additional constraint of concentration symmetry further

improvements in the velocity accuracy were obtained. The improved VCPIV algorithm is the first micro PIV method that can measure particle concentration in the z-direction, which has many applications in the study of particle migration phenomenon in industrial processes and bio-flows.

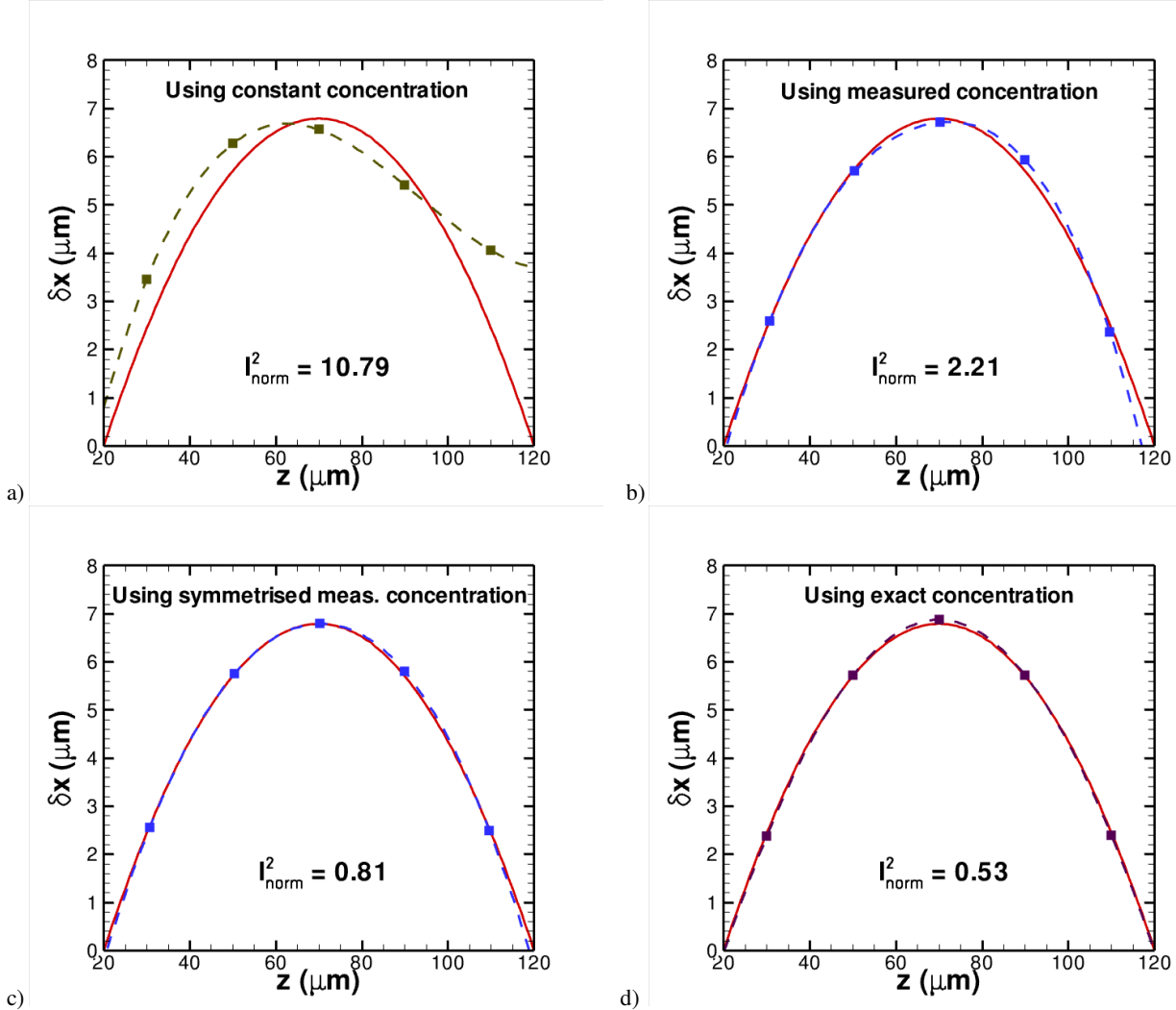


Figure 6. Calculations of velocity profiles through the measurement depth. Solid line represents the exact velocity profile. Squares represent the nodes for the spline solution (dashed lines). a) Velocity profile measured using a uniform concentration. b) Velocity profile measured using the measured concentration profile. c) Velocity profile measured using the measured concentration profile and assuming symmetry. d) Velocity profile measured using the exact concentration. The I_{norm}^2 values represent the total measurement error across the measurement volume.

REFERENCES

- [1] Bitsch, L., Olesen, L., Westergaard, C., Bruus, H., Klank, H. & Kutter, J. (2005) Micro particle-image velocimetry of bead suspensions and blood flows. *Exp Fluids* **39**: 507-513.
- [2] Cao, J. & Wereley, S.T. (2006) Micro-particle image velocimetry in biomedical applications. In *Encyclopedia of Biomaterials and Biomedical Engineering*, editors G. L. Bowlin and G. Wnek, Informa Healthcare, 1873-1884.
- [3] Fouras, A., Lo Jacono, D., Nguyen, C. & Hourigan, K. (2009) Volumetric correlation PIV: a new technique for 3D velocity vector field measurement. *Exp Fluids*, online.
- [4] Lindken, R., Westerweel, J. & Wieneke, B. (2006) Stereoscopic micro particle image velocimetry. *Exp Fluids* **41**: 161-171.
- [5] Meinhart, C.D., Wereley, S.T. & Gray, M. H. B. (2000) Volume illumination for two-dimensional particle image velocimetry. *Meas Sci Technol* **11**: 809-814.
- [6] Nguyen, C.V., Fouras, A. & Carberry, J. (2008) Improved accuracy of micro PIV measurement using image overlapping technique. *14th Int Symp on Applications of Laser Techniques to Fluid Mechanics*, Lisbon, Portugal, 07-10 July.
- [7] Olsen, M.G. & Adrian, R.J. (2000) Out-of-focus effects on particle image visibility and correlation in microscopic particle image velocimetry. *Exp Fluids* **29**: S166-S174.